Assessment of EEG Event-Related Desynchronization in Stroke Survivors Performing Shoulder-Elbow Movements

Michael J. Fu
Electrical Engineering and Computer Science
Case Western Reserve University
Cleveland, Ohio 44106
Email: mjfu@case.edu

Janis J. Daly
Cleveland FES Center
Louis Stokes Cleveland
Dept. of Veterans Affairs
Medical Center
Cleveland, Ohio 44106
Email: jjd17@case.edu

M. Cenk Çavuşoğlu
Electrical Engineering and Computer Science
Case Western Reserve University
Cleveland, Ohio 44106
Email: cavusoglu@case.edu

Abstract—It is unknown whether electroencephalography (EEG) signal characteristics in stroke survivors with motor deficits register enough activity for use with brain-computer interfaces (BCIs). This research studied pre-movement EEG from shoulder-elbow movement in stroke survivors to identify signal characteristics potentially useful for robot-assisted stroke rehabilitation. Pre-movement event-related desynchronization (ERD) was examined in the alpha band mu rhythm for control (n = 7) and stroke subjects (n = 11). Subjects were all right-hand dominant; stroke subjects used their impaired arm and controls were assigned a side to match stroke subjects. Both non-dominant-arm-tested stroke and control subjects exhibited greater ERD intensity vs. those using their dominant arm ($p < 0.05$). Also, pre-movement ERD was detected in stroke survivors, which suggests at the possibility of using ERD as a BCI system control signal. However, the peak ERD of stroke survivors was significantly lower than that of healthy subjects ($p < 0.05$), which brings doubt to whether the intensity of ERD in stroke survivors is large enough to be used as a BCI system control signal.

I. INTRODUCTION

Of the many complex processes that occur in the human brain, cortical activity that drives motor-related cognitive planning has become an important field of research for studies attempting to decode the brain's electrical activity for use as a control signal in brain-computer interfaces (BCIs) or brain-machine interfaces (BMIs). Many studies reported the use of BCI or BMI to improve the lives of people paralyzed by spinal chord injuries (SCI) or amyotrophic lateral sclerosis (ALS) - individuals who can plan out or imagine movements normally, but not perform them [1]. In these studies, BCI systems detected and translated the brain's neural activity into prosthesis control signals or into mouse cursor motions for communication purposes [2]. Stroke survivors, however, differ from SCI or ALS afflicted individuals because stroke-related motor deficits can be rehabilitated to a greater degree than total paralysis. Therefore, stroke survivors could benefit from BCI not as a permanent prosthesis-driving technology, but instead as a rehabilitation tool.

A BCI system can be paired with a rehabilitation robot to provide adaptive therapies to motor-impaired stroke survivors. Such a combination has the potential to outperform classical methods in providing functional recovery and promoting cortical plasticity. By plasticity, we refer to the brain's ability to reorganize around damaged cortical areas and recover functions that those areas were once responsible for. Using EEG recordings, Sterns, et al. discovered that increases in task-related coupling between cortical areas may compensate for brain damage after stroke [3]. They also found that some of the increased coupling decreases as patients make a functional recovery. If a BCI system can identify motor-related activity in stroke survivors using electroencephalography (EEG), it can then control a rehabilitation robot to adapt therapy sessions to promote plasticity in the brain of the subject.

Since the 1990s, rehabilitation robots have been an effective component of stroke therapy studies [4]. Unlike a self-evoked motion, robots like the Interactive Motion Technologies Inc. (Cambridge, MA) Inmotion² Shoulder-Elbow Robot (Fig.1) challenge and assist stroke survivors to accomplish movements they cannot otherwise successfully perform. Lum, et al. found that robot-assisted therapy helped stroke survivors improve more in both functional and biomechanical measures than conventional therapy [5]. A combination of robotic rehabilitation and BCI would allow therapists to actively measure and restore lost motor skills cortically, instead of only functionally.

However, because of the ischemia, damaged neurons, and potentially altered neural activity, it is unknown whether EEG in stroke survivors is compatible with BCI systems. Also, existing studies of EEG in stroke survivors only examine finger movements or motor tasks that the stroke subjects were able to successfully perform [7]. Rehabilitation robots such as the Inmotion² are designed to target the movement of larger muscle groups, such as shoulder-elbow motions, but the EEG characteristics related to a shoulder-elbow movement in healthy adults and stroke survivors is unknown.
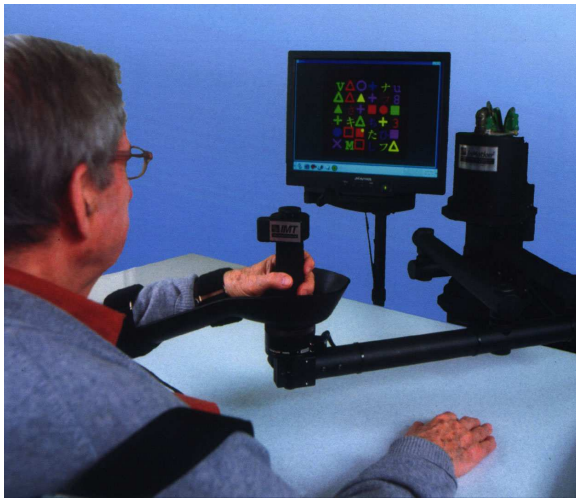
Fig. 1. The Inmotion[2] Shoulder-Elbow Robot is used in upper extremity physical rehabilitation therapies and only allows 2D shoulder-elbow movements [6].

Fig. 2. The relative locations of the 64-electrode International 10-20 EEG electrode placement standard used in this study [8].

A. Study Objectives

The purpose of this research was to characterize pre-movement EEG from a shoulder-elbow movement in stroke survivors in order to identify signal characteristics that could potentially be used in BCI applications. Also, this study extended existing literature in a number of ways. First, we provided the alpha band mu rhythm event-related desynchronization (ERD) characteristics of stroke-affected EEG during a shoulder-elbow motion (with the Inmotion[2] Shoulder Elbow Robot in Fig. 1). Second, we provided new information regarding alpha-mu ERD characteristics for dominant versus non-dominant shoulder elbow movements for both healthy control subjects and stroke survivors.

B. Paper Outline

First, the background section provides reviews of topics relevant to this study. Then, we described the experiment procedures and data analysis methods. The results section highlights key results from this study (in terms of peak electrode locations, average mu frequency, and peak ERD%) and we concluded with discussions and future work for our findings.

II. Background

A. Brain Computer Interface

BCI systems are designed to translate the brain's activity during imagined movements into computer cursor or pros-thesis control. Wolpaw, *et al.* at the Wadsworth Center for Laboratories and Research in NY implemented a pioneering EEG-based BCI system in 1991 [9]. This system measured the amplitude of mu waves to allow a well-trained subject to control the direction of a cursor in one dimension by varying the amplitude of their mu waves [9]. In 2004, the same group was able to make two dimensional control possible using scalp-recorded EEG, even though it was widely assumed
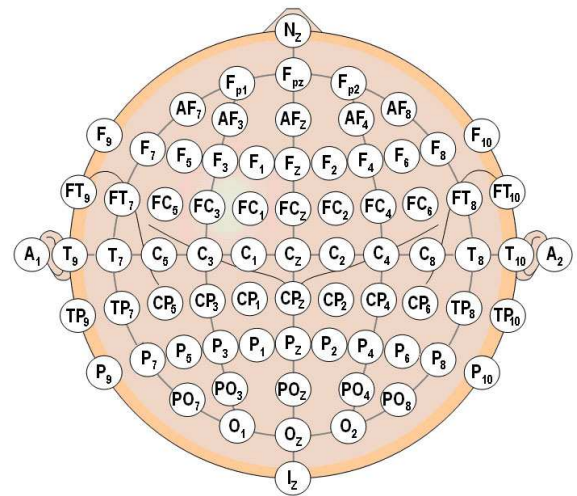
that only invasive recordings of brain waves can provide the resolution needed to achieve 2D control [10].

These advancements in noninvasive EEG BCI systems are important for developing a BCI system for stroke survivors because invasive recordings require implanted electrodes under the skull, which is not desirable for individuals who already have stroke-induced damage to their brains.

B. Alpha Band Mu Rhythm

The alpha band of EEG waves is defined to be the frequency band between 8–12 Hz. Included in the alpha band, there are mu rhythms that are closely related to cortical motor planning. Mu stands for "motor" and in most healthy adult subjects the mu wave is attenuated whenever voluntary, passive, or reflexive movements are performed or even imagined. Mu rhythm attenuation occurs up to, and sometimes beyond, 2 s before movement onset in healthy adults and has key harmonically independent frequency components at around 10 Hz (alpha component) and at 20 Hz [11]. The alpha component can exist anywhere from 8 Hz to above 11 Hz in some adults and arises from the sensory cortex, so it is usually most active and detectable at electrode sites that overlay this cortical area (the C and CP electrodes in Fig. 2). Attenuation of mu rhythms occurs prior to and during movements, which is also called desynchronization [12].

C. Event-Related Desynchronization

Event-related desynchronization refers to desynchronization that occurs due to voluntary or involuntary activity. It is also a reliable correlate of increased cellular excitability in the thalamocortical systems during cortical information processing [11]. In contrast, when the brain is idling (at rest), alpha waves are enhanced, reflecting greater amplitudes in the EEG data. One theory on the cause of desynchronization is that neurons behave like weakly-coupled non-linear oscillators which synchronize with each other when the brain is idle,
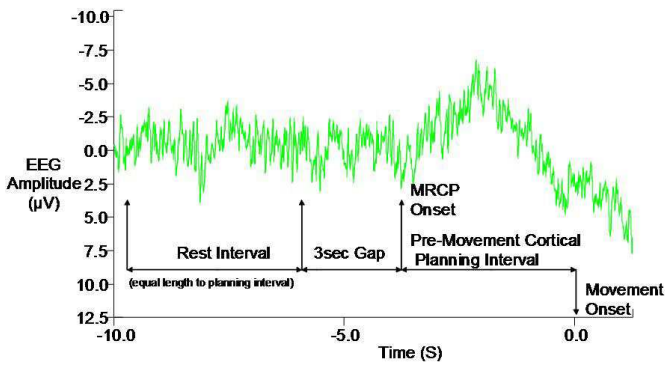
Fig. 3. Diagram showing a healthy adult's EEG during a shoulder-elbow movement with corresponding MRCP (the negative potential between the labels 'MRCP Onset' and 'Movement Onset'). The rest and planning intervals are also shown as defined for stroke subjects.

but desynchronize from the weak coupling when processes become active in the brain [13].

To quantify the amount of EEG desynchronization, we compute the percent of event-related desynchronization, defined by:

$$ERD\%_{decrease} = 100 \times \frac{M_{ref} - M_x}{M_{ref}} \qquad (1)$$

where M_{ref} is the average power in a reference interval (typically a period of time lasting a few seconds while the subject is at rest) and M_x is the average power in an interval of interest with which we wish to compare the reference interval for activity in the EEG data. A positive ERD percentage indicates that there is a decrease in power with respect to the reference state and a negative value means there is an increase in power.

D. Movement-Related Cortical Potentials

Besides ERD, there is also movement-related EEG activity in the slow, 0.1–1 Hz range called the movement-related cortical potential (MRCP). MRCPs are negative potentials that can be seen in the raw EEG data after averaging many trials of the same motor task together (Fig 3). The start of the MRCP curve is believed to be the onset of pre-motor planning and the amplitude of the curve is correlated to the amount of cognitive effort. Although the MRCP reflects cortical activity, it is not practical as a BCI input signal because it is discernable only after averaging many trials, unlike ERD. However, MRCP and ERD share common timing characteristics, so MRCP start times and duration can be used to help identify periods of cortical activity in which ERD should be present [14].

III. Experiment Procedures

A. Subjects

Twenty right-hand-dominant subjects were selected and gave consent to enroll in this study. This study was conducted according to the Declaration of Helsinki and oversight was provided by the IRB of the Louis Stokes Cleveland Veterans Affairs Medical Center. Ages ranged from 48–72 years old, with a mean age of 61. Twelve of these subjects had chronic

(> than 12 months) arm coordination deficits following stroke and eight subjects were age-matched, healthy individuals.

B. Experiment Paradigm

All of the subjects were seated before a computer screen with either their right or left hand gripping the end-effector of an Inmotion[2] Shoulder Elbow Robot. Control subjects were randomly assigned to use their left or right arm while stroke survivors used the arm suffering coordination deficits. The subjects were then presented with a motor targeting task that required an accurate 14 cm, linear movement in the horizontal plane beginning at the center of the workspace and moving to a target in a direction directly in front of the subject. This motor task requires shoulder flexion and elbow extension, which each subject performed 50 times with a 2 minute recess between every 10 trials. Not all stroke survivors could accomplish the motor task, but all of them made their best effort to do so.

C. Data Acquisition

Simultaneous data recordings were obtained for EEG, electromyography (EMG), and movement onset (with a custom goniometric device). EEG data was obtained using Compumedics NeuroScan Ltd. (El Paso, TX) devices and software. The data was recorded using Acquire 4.3.1 software, a 64-electrode Quick-Cap EEG cap, and a Synamps amplifier system (500 gain, sampling rate of 1000 Hz, bandpass filter 0.1–40 Hz). All electrodes on the EEG cap were 8 mm in diameter with a 5 mm cavity depth and were arranged on the scalp in compliance with the International 10-20 standard [15]. Each recording was referenced to the common linked left and right mastoid surface electrodes. All electrode-to-scalp impedances were reduced to less than 10 kΩ using electrically conductive gel and real-time electrode impedance measurements provided by the Acquire software.

IV. Data Analysis Methods

The EEG data was first examined and filtered for noise. Then, we optimized the SNR of the EEG data by using spatial filtering and searched for any contamination by scalp or facial muscle EMG signals. Finally, we analyzed the locations of greatest brain activity and the corresponding amounts of peak ERD% during pre-movement motor planning.

A. Noise Rejection

The EEG data was first visually inspected by an expert to reject trials containing blink artifacts or abnormalities in the baseline data. Upon further analysis, an unknown noise source with a center frequency at 20 Hz was observed in all of the subjects' data. The noise existed approximately between 19–21 Hz and was non-uniformly distributed across the electrode locations. To suppress the noise, we applied a 48 dB/octave bandstop filter from 19–21 Hz. However, because the beta band component of mu waves in normal adults is most active at approximately 20 Hz, the noise prevented accurate analysis of the beta band for cortical activity [11]. Therefore analysis was performed only on the alpha band for this study.

B. Spatial Filtering

Using NeuroScan Edit 4.3.1, a common average reference (CAR) was performed on all 64 electrodes in order to produce a "reference-free" version of the EEG data. CAR was chosen base on its superior SNR characteristics as reported in a study performed by McFarland, which compared several spatial filtering techniques for improving the SNR of EEG signals for BCI use and concluded that the CAR had the best SNR [16]. In the calculation of the CAR, the average value of all 64 electrodes is subtracted from the channel of interest for each sample of data. Specifically, the formula for CAR was:

$$V_i^{CAR} = V_i^{ER} - \frac{1}{64} \sum_{j=1}^{64} V_j^{ER} \qquad (2)$$

where V_i^{ER} is the potential between the ith electrode and the reference electrode. The effect of the CAR spatial filter was that any noise common to all the electrodes was reduced from the EEG data.

C. Scalp and Facial Muscle EMG Noise Rejection

We observed that some of the stroke survivors exerted considerable effort while attempting the motor task, which lead to the possibility that their facial muscles were strained or teeth were clenched. These muscle contractions introduce EMG activity that could be sensed by the EEG electrodes and subsequently recorded along with cortical activity.

The following methods for EMG detection are largely based on the results of a study by Goncharova on the characteristics of facial and scalp muscle EMG signals as measured through EEG recording equipment [17]. The EMG detection and rejection were done for both the pre-movement planning interval and the rest interval of each trial because EMG noise in either interval would have decreased the accuracy of ERD calculations. The planning state was approximated as the 3 s interval preceding movement onset and the rest state was a separate 3 s interval preceding the planning state.

EMG from the frontalis and temporalis muscles can be a source of noise when examining EEG signals because the range of frequencies spanned by EEG and EMG overlap. Clinically relevant scalp EEG signals range from 0.1–100 Hz, but EMG exists from 0 to >200 Hz [11]. The frontalis muscle (which moves the eyebrows) shows maximum EMG activity from 20–30 Hz and the temporalis muscles (which are contracted when teeth are clenched) have maximum EMG activity from 45–70 Hz. Even with weak contractions, EMG data is detectable at the vertex of the scalp in the 8–12 Hz frequency band (exactly our frequencies of interest), so it was important to reject any trial suspected of having EMG signals from the frontalis or temporalis muscles.

To determine whether a trial might contain EMG noise, data was analyzed from 4 electrode locations that were most susceptible to EMG contamination, which will be referred to as the "primary" electrodes for EMG rejection. AF7 and AF8 are most affected by the frontalis muscles, and FT7 and FT8 are most affected by the temporalis muscles [17]. At

these electrodes, the 45–70 Hz frequency band power was first computed in each trial because scalp muscle EMG exhibits peaks in this frequency band, but EEG signals do not. The power was calculated using the formula:

$$Power_{45-70Hz} = \frac{1}{N^2} \sum_{k=\frac{45N}{f_s}}^{\frac{70N}{f_s}} \left(|X(k)|^2 + |X(N-k)|^2 \right) \quad (3)$$

where N is the total number of samples in the rest or planning state and $X(k)$ is the kth FFT coefficient, and f_s is the sampling frequency.

In any of the 50 trials, if the 45–70 Hz band power for a primary electrode exceeded one standard deviation above the 50-trial mean for each respective electrode, then five immediately adjacent electrodes were analyzed. The goal was to determine if the 45–70 Hz power value from the same trial at adjacent electrodes also exceeded the mean plus one standard deviation. Finally, if three of the five adjacent electrodes had power values that exceed one standard deviation above the mean, then the suspected trial was rejected from analysis.

We experimentally chose to use three adjacent electrodes as the decisive number. EEG data was recorded from a healthy adult performing the experimental motor task with and without intentional frontalis and temporalis muscle contractions. Then, a dataset of 50 trials was randomly created out of 36 EMG-free trials and 14 frontalis and temporalis EMG-contaminated trials in order to test the EMG detection algorithm described above. The algorithm performed best using 3 adjacent electrodes as the decisive number and rejected 6 of the 14 contaminated trials. Using 4 and 5 adjacent electrodes as the decisive number resulted in detection of only 4 of the same 14 contaminated trials.

Mean plus one standard deviation was chosen as a threshold in the algorithm because we found that rejecting trials outside this threshold preserved roughly 85% of uncontaminated data, 20% of frontalis contaminated data, and 0% of frontalis and temporalis contaminated data.

V. ERD DATA PROCESSING

For each subject, the ERD% for each trial was computed and averaged. Matlab, Compumedics NueroScan Edit 4.3.1, and procedures consistent with existing literature were used [11].

First, the electrode with greatest alpha band pre-movement activity was identified. Subsequently, the frequency component in the alpha band with the greatest change in amplitude was identified as the mu frequency. Next, the data was bandpass filtered at the mu frequency $\pm$ 1 Hz, all the accepted trials of data were averaged, and the ERD percentage value is calculated for each sample of data.

The electrode with the greatest pre-movement planning activity was identified by comparing the average power of a subject's rest state to their planning state for the alpha band. For control subjects the motor planning state was identified as the period 2 s preceding movement onset while the rest state was a 2 s interval that began 5 s before the

active interval. These periods were identified using the MRCP timing characteristics for each subject, which identified when cortical planning began. The mean MRCP start time for the control subjects occurred 1.466 ± 779 ms (approximately 2 s) before movement onset [18]. For stroke survivors performing a shoulder-elbow movement, Daly, et al. found that the average sensorimotor MRCP start time (2.734 ± 1.205 ms) varied much more than that of the control subjects. In light of this fact, the active state for stroke subjects was chosen to be the time between the start of the MRCP and movement onset [18]. The rest interval was chosen as an interval equal in length to the active interval and ended 3 s before the start of the active interval, as seen in Fig. 3.

Matlab's periodogram function was used to compute the power spectral density (PSD) in the alpha band for electrodes overlaying the sensorimotor cortex (FCZ, FC1-6, CZ, C1-6, CPZ, and CP1-6). The level of activity at an electrode was computed by subtracting the rest PSD from the active PSD and integrating over all frequency components from 8–12 Hz. The electrode with the greatest difference in power was identified as the one with peak activity. We excluded the data of two subjects from analysis because their data did not show desynchronization in the alpha band.

The individual frequency component where activity peaks was identified at the peak electrode by finding the frequency in the alpha band that exhibited the greatest change in amplitude between the rest and active state.

ERD% was then calculated for the alpha band mu frequency $\pm$ 1Hz using the Event Related Band Power (ERBP) function in NeuroScan Edit 4.3.1.

Statistical Analysis

Each subject's peak ERD% during the planning interval was recorded and used as the independent variable in a series of analyses of variance (ANOVA). One-way ANOVA models were analyzed for dominant (right-arm-tested) control vs. stroke subjects, non-dominant (left-arm-tested) control vs. stroke subjects, and for all control vs. all stroke subjects.

VI. RESULTS

A. Brain Region and Frequency of Greatest Activity

In a normal adult performing a single-handed motor-task, the greatest motor-related cortical activity will occur at approximately 10 Hz on the side of the brain contralateral to the side of motion, which we will refer to as the "working side" [11]. Electrodes directly overlaying or adjacent to the motor cortex (FC, C, and CP electrodes) on the working side of the brain are commonly the most active, though it is not uncommon for the medial Z electrodes to be equally as active.

We noted from Table I that 5 of the 7 Control subjects showed peak activity at electrode locations on the working side of the brain, four of which occur at CP electrodes. It is unknown why subjects number 4 and 6 exhibited more activity on the non-working side. In general, the control subjects showed the greatest activity in the central-parietal region of the brain.

TABLE I

RESULTS OF DATA ANALYSIS

Subject No.	Peak Electrode	Mu (Hz)	Peak ERD (%)
A) Control - Dominant (Right) Arm Tested			
1.	CPZ	8.5	72.0
2.	CP5	10.0	63.6
4.	C6	8.0	47.4
8.	C5	10.0	55.8
Mean		**9.1 ($\pm$1.0)**	**59.7 ($\pm$10.5)**
B) Stroke - Dominant (Right) Arm Tested			
10.	C6	11.4	45.1
12.	FC1	8.2	30.6
16.	FC6	8.0	48.1
18.	CZ	8.5	47.1
19.	C6	9.0	64.8
20.	FC5	8.5	42.8
Mean		**8.9 ($\pm$1.0)**	**46.4 ($\pm$11.0)**
C) Control - Non-Dominant (Left) Arm Tested			
3.	CP2	9.0	96.7
6.	FC5	8.0	81.9
7.	CP6	10.4	93.2
Mean		**9.1 ($\pm$1.2)**	**90.6 ($\pm$7.7)**
D) Stroke - Non-Dominant (Left) Arm Tested			
9.	C6	11.2	57.5
11.	FC1	9.5	52.2
13.	FC6	9.7	77.8
14.	CZ	8.0	80.1
17.	C6	8.2	64.2
Mean		**9.3 ($\pm$1.3)**	**66.4 ($\pm$12.3)**

The 'Peak Electrode' column is the electrode location at which the greatest pre-movement activity occurred. The 'Mu' column reports the frequency at which there was the greatest difference in amplitude between rest and motor-planning state PSDs. The 'Peak ERD' column reports the greatest amount of ERD in the pre-movement planning state for each subject. Also provided are the mean and standard deviation values for the 'Mu' and 'Peak ERD' data. A) and B) are both dominant-arm-tested subjects while C) and D) are both non-dominant-arm-tested subjects.

In contrast, only 4 of the 11 stroke survivors exhibited peak electrode activity on the working side of the brain. Also, 6 of these subjects had peak activity in the fronto-central brain region. These results showed that the stroke survivors differ from the expected peak pre-movement mu rhythm activity locations.

We also noted that both stroke and control subjects had mu frequencies identified at approximately 9 ($\pm$ 1) Hz, which was within the expected healthy adult norms.

B. Peak Event-Related Desynchronization

The peak ERD% at the mu frequency was determined by finding the greatest ERD% in the interval of time between the onset of the MRCP and movement onset. The onset of the MRCP reflects the beginning of motor planning and the timing of ERD and MRCP coincide, so any ERD occurring in this time interval reflected cortical activity most relevant to

motor planning of the motor task [14].

First we examined the effect of handedness on control subjects. The mean peak ERD% for right-arm-tested control subjects was 59.7 ($\pm$ 10.5)% and the range was 41.4–71%. For left-arm-tested control subjects, the mean ERD peak was 90.6 ($\pm$ 7.7)% with a range of 81.9–96.7%. The ranges of the left and right-arm-tested control subjects did not overlap and an ANOVA model showed that they were significantly different (p = 0.008).

Then, we examined the effect of handedness on stroke survivors. Right-arm-tested subjects had a mean peak ERD of 46.4 ($\pm$ 11)% and a range of 42.8–64.8% while left-arm-tested stroke subjects had a mean peak ERD of 66.4 ($\pm$ 12.3)% with a range of 52.2–80.1%. An ANOVA model revealed a significant difference between the left and right-arm-tested stroke survivors (p = 0.01).

Next, we examined the effect of stroke on the dominant-arm group and found that control subjects who used their dominant arm did not have significantly greater peak ERD% than post-stroke subjects who used their dominant arm (p = 0.09). However, we performed a statistical power analysis and found that $p < 0.05$ could have been achieved if we had 30 dominant arm subjects.

For the non-dominant-arm group, all of the stroke survivors had peak ERD% below the range of the left-arm-tested control subjects. An ANOVA model confirmed that there is a significant difference between the left hand tested stroke and control groups (p = 0.02).

Finally, an ANOVA model for all 7 control subjects vs. all 11 stroke survivors revealed a statistically significant difference between the control and stroke groups (p = 0.04).

VII. Discussion

These results extended existing literature about the effects of hand dominance on pre-movement brain activity. Current studies show that there is more pre-movement cortical activity in healthy adults for non-dominant hand finger movements versus the dominant hand [12], [19], [20]. Specifically, Stancak [12] and Bai [20] both found that ERD occurs at significantly higher percentages for healthy adults moving fingers on the non-dominant hand versus the dominant hand.

We showed that the effect of hand dominance on ERD% for shoulder-elbow motion is consistent with literature; both control and stroke subjects showed significantly higher peak ERD% when the non-dominant arm was tested versus the dominant arm ($p < 0.05$).

This observation showed that handedness significantly influences pre-movement brain activity for shoulder-elbow motion in stroke survivors and highlights hand-dominance as an important independent variable in the design of future experiments on stroke survivors.

VIII. Conclusion

The present research study found that a certain amount of pre-movement ERD is detectable in stroke survivors for shoulder-elbow movement. This finding suggests that it might be possible to use ERD as a BCI system control signal for robot-assisted rehabilitation of stroke survivors. However, the peak ERD% of stroke survivors was found to be significantly lower than that of healthy subjects, which brings doubt to whether the intensity of ERD in stroke survivors is large enough to be used as a BCI system control signal. This requires further studies.

Future Work

Due to the limitations of this study, the beta band component of mu waves could not be studied, but it is known to exhibit ERD during pre-motor cortical planning in the hand movements of healthy adults and in stroke survivors [7], [11]. Therefore, an investigation into the behavior of shoulder-elbow pre-movement ERD is one area of future study.

In addition to mu waves, high-frequency EEG waves are also known to reflect cortical activity, but have yet to be studied in stroke survivors. A study on monkeys by Heldman has reported that waves of frequencies ranging from 31–200 Hz (high frequency waves) contain signal characteristics that can be used to predict arm velocities during a circle drawing task (high frequency waves were not analyzed in this study because amplifier filters were set to cutoff frequencies above 40 Hz) [21]. Heldman's study used intracortical electrodes, which have much higher frequency resolution than scalp-mounted electrodes, but scalp electrodes are routinely used to study frequencies up to 100 Hz and even higher-frequency recordings are recommended by the emerging Full-band EEG (FbEEG) recording standard [11], [22]. Investigations of high-frequency EEG characteristics in stroke survivors do not exist in literature, but this is an area of future study with potentially important findings.

Acknowledgment

References

[1] R. B. Stein, "Summing up," June 2005, addressed to Brain-Computer Interface Technology, 3rd International Meeting, The Rensselaerville Institute, Rensselaerville, NY.

[2] J. Wolpaw, N. Birbaumer, D. J. McFarland, G. Pfurtscheller, and T. M. Vaughan, "Brain-computer interfaces for communication and control," *Clinical Neurophysiology*, vol. 113, pp. 767–791, June 2002.

[3] L. Sterns, P. Asselman, A. Pogosyan, C. Loukas, A. J. Thompson, and P. Brown, "Corticocortical coupling in chronic stroke: its relevance to recovery," *Electroencephalography and Clinical Neurophysiology*, vol. 63, pp. 475–484, August 2004.

[4] R. Riener, T. Nef, and G. Colombo, "Robot-aided neurorehabilitation of the upper extremities," *Medical and Biological Engineering and Computing*, vol. 43, pp. 2–10, January 2005.

[5] P. S. Lum, C. G. Burgar, P. C. Shore, M. Majmundar, and M. Van der Loos, "Robot-assisted movement training compared with conventional therapy techniques for the rehabilitation of upper-limb motor function after stroke," *Archives of Physical Medicine and Rehabilitation*, vol. 83, pp. 952–959, June 2002.

[6] Interactive Motion Technologies Inc., "Interactive motion technologies product description pamphlet," Cambridge, MA, 2004.

[7] T. Platz, I. H. Kim, H. Pintschovius, T. Winter, A. Kieselbach, K. Villringer, K. R., and K. Mauritz, "Multimodal EEG analysis in man suggests impairment-specific changes in movement-related electric brain activity after stroke," *Brain*, vol. 123, pp. 2475–2490, December 2000.

[8] J. Malmivuo and R. Plonsey, *Bioelectromagnetism*, 1st ed. New York, New York: Oxford University Press, 1995.

[9] J. Wolpaw, D. J. McFarland, G. W. Neat, and C. A. Forneris, "An EEG-based brain-computer interface for cursor control," *Electroencephalography and Clinical Neurophysiology*, vol. 78, pp. 252–259, March 1991.

[10] J. Wolpaw and D. J. McFarland, "Control of a two-dimensional movement signal by a noninvasive brain-computer interface in humans," *Proceedings of the National Academy of Sciences*, vol. 101, pp. 17 849–17 854, December 2004.

[11] E. Niedermeyer and L. H. Lopes da Silva, *Electroencephalography: Basic Principles, Clinical Applications, and Related Fields*, 4th ed. Baltimore, MD: Williams and Wilkins, 1999.

[12] A. J. Stancak and G. Pfurtscheller, "The effects of handedness and type of movement on the contralateral preponderance of mu-rhythm desynchronisation," *Electroencephalography and Clinical Neurophysiology*, vol. 99, pp. 174–182, August 1996.

[13] W. S. Newman, November 2005, personal communication.

[14] C. Toro, G. Deuschl, R. Thatcher, S. Sato, C. Kufta, and M. Hallet, "Event-related desynchronization and movement-related cortical potentials on the ECoG and EEG," *Electroencephalography and Clinical Neurophysiology*, vol. 93, pp. 380–389, October 1994.

[15] H. H. Jasper, "Report of the committee on methods of clinical examination in electroencephalography," *Electroencephalography and Clinical Neurophysiology.*, vol. 10, pp. 370–375, 1958.

[16] D. J. McFarland, L. M. McCane, S. V. David, and J. R. Wolpaw, "Spatial filter selection for EEG-based communication," *Electroencephalography and Clinical Neurophysiology.*, vol. 103, pp. 386–394, September 1997.

[17] I. I. Goncharova, D. J. McFarland, T. M. Vaughan, and J. R. Wolpaw, "EMG contamination of EEG: spectral and topographical characteristics," *Clinical Neurophysiology*, vol. 114, pp. 1580–1593, March 2003.

[18] J. J. Daly, Y. Fang, E. M. Perepezko, V. Siemionow, and G. Yue, "Prolonged cognitive planning time, elevated cognitive effort, and relationship to coordination and motor control following stroke," 2004, abstract submitted for review.

[19] I. M. Tarkka and M. Hallet, "Cortical topography of premotor and motor potentials preceding self-paced, voluntary movement of dominant and non-dominant hands," *Electroencephalography and Clinical Neurophysiology*, vol. 75, pp. 36–43, February 1990.

[20] O. Bai, Z. Mari, S. Vorbach, and M. Hallett, "Asymmetric spatiotemporal patterns of event-related desynchronization preceding voluntary sequential finger movements: a high-resolution eeg study," *Clinical Neurophysiology*, vol. 116, pp. 1213–1221, March 2005.

[21] D. A. Heldman, W. Wang, S. S. Chan, and D. W. Moran, "Local field potential spectral tuning in motor cortex during reaching and drawing movements," Society for Neuroscience Abstracts, October 2004, presented in San Diego, CA October 23-27.

[22] S. Vanhatalo, J. Voipio, and K. Kaila, "Full-band EEG (FbEEG): an emerging standard in electroencephalography," *Clinical Neurophysiology*, vol. 116, pp. 1–8, January 2004.